International Journal of Nanomedicine

Dovepress
open access to scientific and medical research

Open Access Full Text Article

ORIGINAL RESEARCH

Blockage of both the extrinsic and intrinsic pathways of diazinon-induced apoptosis in PaTu cells by magnesium oxide and selenium nanoparticles

This article was published in the following Dove Press journal:
International Journal of Nanomedicine
22 November 2016
Number of times this article has been viewed

Mahdi Shiri[1,2,*]
Mona Navaei-Nigjeh[1,3,*]
Maryam Baeeri[1]
Mahban Rahimifard[1]
Hossein Mahboudi[4]
Ahmad Reza Shahverdi[5]
Abbas Kebriaeezadeh[1]
Mohammad Abdollahi[1,6,7]

[1]Department of Toxicology and Pharmacology, Faculty of Pharmacy and Pharmaceutical Sciences Research Center, Tehran University of Medical Sciences, [2]School of Medicine, Artesh University of Medical Sciences, [3]Department of Tissue Engineering, School of Advanced Technologies in Medicine, Tehran University of Medical Sciences, Tehran, Iran; [4]Department of Biotechnology, Faculty of Advanced Technologies in Medicine, Shahid Beheshti University of Medical Sciences, Tehran, Iran; [5]Department of Biotechnology, Faculty of Pharmacy and Biotechnology Research Center, [6]Toxicology Interest Group, USERN, [7]Endocrinology & Metabolism Research Institute, Tehran University of Medical Sciences, Tehran, Iran

*These authors contributed equally to this work

Correspondence: Mohammad Abdollahi
Department of Toxicology and Pharmacology, Faculty of Pharmacy and Pharmaceutical Sciences Research Center, Tehran University of Medical Sciences, Poursina Avenue, Tehran 1417614411, Iran
Email mohammad@tums.ac.ir

Abstract: Diazinon (DZ) is an organophosphorus insecticide that acts as an acetylcholinesterase inhibitor. It is important to note that it can induce oxidative stress, lipid peroxidation, diabetic disorders, and cytotoxicity. Magnesium oxide (MgO) and selenium nanoparticles (Se NPs) showed promising protection against oxidative stress, lipid peroxidation, cytotoxicity, and diabetic disorders. Therefore, this study was conducted to explore the possible protective mechanisms of MgO and Se NPs against DZ-induced cytotoxicity in PaTu cell line. Cytotoxicity of DZ, in the presence or absence of effective doses of MgO and Se NPs, was determined in human pancreatic cancer cell line (PaTu cells) after 24 hours of exposure by using mitochondrial activity and mitochondrial membrane potential assays. Then, the insulin, proinsulin, and C-peptide release; caspase-3 and -9 activities; and total thiol molecule levels were assessed. Determination of cell viability, including apoptotic and necrotic cells, was assessed via acridine orange/ethidium bromide double staining. Furthermore, expression of 15 genes associated with cell death/apoptosis in various phenomena was examined after 24 hours of contact with DZ and NPs by using real-time polymerase chain reaction. Compared to the individual cases, the group receiving the combination of MgO and Se NPs showed more beneficial effects in reducing the toxicity of DZ. Cotreatment of PaTu cell lines with MgO and Se NPs counteracts the toxicity of DZ on insulin-producing cells.

Keywords: apoptosis, diazinon, human pancreatic cancer cell line, organophosphorus, toxicity

Introduction

Diazinon (DZ) is an organophosphorus (OP) insecticide that acts as an acetylcholinesterase (AChE) inhibitor. AChE inhibition results in accumulation of acetylcholine in the synaptic cleft. When DZ enters the body, it can be oxidatively degenerated to diazoxon in the liver microsomal enzyme system by using NADH and O_2.[1] Diazoxon, an active oxygen metabolite of DZ, causes predictably higher levels of AChE inhibition than the parent compound owing to the fact that the parent compound does not inhibit AChE directly.[2–4] In addition, studies have indicated that DZ could increase the generation of reactive oxygen species (ROS), mitochondrial membrane damage, oxidative stress, oxidative modifications, lipid peroxidation (LPO) and DNA fragmentation in the genomic DNA content of the tissues/cells to induce cardiotoxicity, neurotoxicity, genotoxicity or cytotoxicity, and apoptosis.[5–9]

RIN, HIT, MIN, INS-1, and beta-TC cells are insulin-producing cell lines that are mostly used in in vitro studies.[10] Although these pancreatic cell lines could produce insulin,

submit your manuscript | www.dovepress.com
Dovepress
http://dx.doi.org/10.2147/IJN.S119680

somatostatin, and glucagon and provide valuable information about physiological, pathophysiological, and differentiation processes, they are derived from rodents, which show some differences from human insulin-producing cells. Hence, there is an emerging need to establish a beta cell line of a human or pig origin. The PaTu cell line is a new source of insulin-producing cells for diabetic patients that has overcome the limited availability of islets for transplantation.[11] It was derived from a human pancreatic Grade II adenocarcinoma of ductal origin.

Metal oxide nanoparticles (NPs) exhibit unique physical and chemical properties due to their limited size and the high density of the corner or edge surface sites. Among various metal oxides, magnesium oxide (MgO) is a functional semiconductor that has multiple applications in drug delivery, pharmaceutics, optoelectronics, cell signaling, and imaging because of its potent antimicrobial and antioxidant properties.[12,13] Previous studies have examined the protective effects of MgO NPs on oxidative stress parameters induced by malathion and chlorpyrifos, the widely used OP.[13,14] It was observed that malathion-induced cardiac cell toxicity is improved by administration of Mg as a result of increasing cardiac adenosine triphosphate (ATP) through active transport of Mg inside the cells. Due to the increasing level of ATP through the liberation of MgO into cells and the improvement of hypoxia, MgO NPs can protect mitochondria against the temporary cardiac arrest.[14] In chlorpyrifos-induced lymphocytes, treatment with MgO NPs could ameliorate the toxic effects of OP pesticide by increasing the viability and decreasing apoptosis, oxidative stress, and inflammation.[13]

Moreover, previous in vitro and in vivo studies have elucidated the protective role of selenium NP (Se NP).[15,16] Thus, this NP is recognized as an antioxidant, cytotoxic, and anti-inflammatory agent. It was demonstrated that Se NPs at a concentration of 250 μg/kg could act as a potent anti-inflammatory agent and could alleviate arthritis-induced parameters. Furthermore, it has been indicated that treatment of arthritic rats with 500 μg/kg dose of Se NPs could restore antioxidant enzyme (superoxide dismutase, glutathione peroxidase, and catalase) levels in liver, spleen, and kidney tissues.[17] In addition, Se NPs supplementation appeared to cause a DNA repair response, which protects DNA from subsequent challenge with DNA-damaging agents.[15]

Given the above evidence, it seems that protective mechanisms of chemically fabricated NPs, such as MgO NPs or biologically produced Se NPs or biogenic ones, are less clear. Therefore, this study aimed to investigate protective mechanisms of MgO and Se NPs against DZ-induced cytotoxicity in PaTu cell line through different methods such as 3-(4,5-dimethylthiazol-2-yl)-2,5-diphenyltetrazolium bromide (MTT) assay, mitochondrial membrane potential (MMP) assay, insulin, proinsulin and C-peptide release activity, caspase-3 and -9 activities, and total thiol molecules (TTM). Determination of cell viability, including the number of apoptotic and necrotic cells, was calculated via acridine orange/ethidium bromide (AO/EB) staining. Furthermore, expression of 15 genes associated with cell death/apoptosis in various phenomena after 24 hours of contact with diazinon and NPs was examined using real-time polymerase chain reaction (PCR).

Materials and methods

Reagents

MgO NPs in the range of 50±5 nm were purchased from the ZFS Company (Yazd, Iran). Se NPs were biosynthesized using *Klebsiella pneumoniae* as described earlier.[18] Diazinon (O,O-diethyl-o-[2-isopropyl-6-methyl-4-pyrimidinyl]-phosphorothioate) was obtained from Shimi-Keshavarz Pesticide Production Company (Tehran, Iran). Likewise, human-specific insulin, proinsulin and C-peptide ELISA kits, and Human Apoptosis RT Array kit were obtained from Mercodia (Uppsala, Sweden) and NanoCinna (Tehran, Iran), respectively. The SYBR green master mix was purchased from Takara (Dalian, People's Republic of China), and TRIzol reagent was obtained from Invitrogen Life Technologies (Karlsruhe, Germany). All the other chemicals were purchased from Sigma-Aldrich (Steinheim, Germany).

Preparation of Se NPs

A bacterial isolate from the Caspian Sea was used for intracellular biosynthesis of the Se NPs according to our previously described method.[18,19] Briefly, sterile nutrient broth medium supplemented with Se^{4+} ions (100 mg/L) was prepared, and 100 mL of this media was transferred to 500 mL Erlenmeyer flask. The medium was inoculated with 1 mL of the fresh inoculums (D_{600} of 0.1) and incubated aerobically at 30°C in a shaker incubator (150 revolutions/min). After 14 hours, the bacterial cells and Se NPs were removed from the culture medium by centrifugation. The pellets were washed, frozen with some liquid nitrogen, and then disrupted using a pestle. The resulting slurry was ultrasonicated and washed three times. The pellets were suspended in deionized water, and the resulting suspension containing Se NPs and cell debris was collected. Then n-octyl alcohol was added, and the mixtures were shaken. The two mixed phases were completely separated by centrifugation and stored at 4°C for 24 hours. After this period of time, the generated Se NPs could be observed at the bottom of the tubes. To ensure that all cell debris was removed, the purified Se NPs were resuspended in the liquid–liquid phase system and were cleaned again.

A stock solution of Se NPs was prepared (1 mg/mL) and used for further biological experiments.

Cell culture

The PaTu cell line was provided by the Pasteur Institute of Iran and was cultured in Roswell Park Memorial Institute (RPMI) 1640 medium containing 10% fetal bovine serum, 100 U/mL penicillin, and 100 µg/mL streptomycin sulfate at 37°C in a 5% CO_2 humidified atmosphere. The medium was exchanged every 2 days. The study was approved by the Institutional Review Board of the Artesh University of Medical Sciences; consent for use of cell lines was obtained by the Pasteur Institute of Iran.

Toxicity of diazinon on PaTu cell line

Before performing test procedures, according to previous studies,[20,21] the PaTu cell lines (1×10^5 cells/well) were incubated with culture medium in combination with different concentrations of DZ (100, 250, 500, 750, 1,000, 1,500, and 2,000 µM) for 24 hours at 37°C in a 5% CO_2 humidified atmosphere. After treatment, the cytotoxicity was assessed using MTT assay. In addition, the probit regression analysis (StatsDirect, Version 3.0.177, Cheshire, UK) was used to estimate the median inhibitory concentration (IC50) of DZ.

Effect of MgO and Se NPs on PaTu cell line

The effect of various concentrations of MgO and Se NPs on the viability of the PaTu cell line was compared to the nontoxic concentrations of MgO and Se NPs as the selective concentrations for the counteraction of DZ-induced cytotoxicity. In previous studies, it was demonstrated that low concentrations (<200 µg/mL) of MgO and Se NPs have no cytotoxicity when examined by MTT assay.[13,19,22,23] In this regard, PaTu cells (1×10^5 cells/well) were exposed to logarithmically increasing concentrations of MgO NPs (0.1, 1, 10, and 100 µg/mL) and Se NPs (0.01, 0.1, 1, 10, and 100 µg/mL) at 37°C in a 5% CO_2 humidified atmosphere. After 24 hours of treatment, the cells were incubated to determine the viability using the MTT assay.

Treatment conditions and experimental groups

On the basis of the results of the pilot studies, DZ at a concentration of 1,300 µM was used to induce cytotoxicity in the PaTu cell line. In this regard, the cell suspension (1×10^5 cells/well) was incubated with culture medium in combination with 1,300 µM DZ for 24 hours at 37°C and 5% CO_2 humidified atmosphere. For protective treatment, 100 µg/mL of MgO NPs and 0.01 µg/mL of Se NPs were used alone and in combination with each other in the presence of the DZ. After a 24-hour interval, the cell suspensions in each group were centrifuged. The supernatants were removed to perform further biochemical assays. The deposited cells were used for viability and cell death assays in the next steps.

Measurement of physiological function of PaTu cell line

Insulin release

Insulin assay was carried out using human-specific insulin ELISA kit (Mercodia) according to the manufacturer's instructions. Briefly, after sample preparation, 10 µL of sample was added into each well followed by addition of 100 µL of enzyme conjugate, and this was then incubated for 2 hours at 25°C. After washing, 200 µL of 3,3′,5,5′-tetramethylbenzidine substrate was added and the wells were incubated for 15 minutes at 25°C in the dark. The process was followed by the addition of 50 µL final solution. The absorbance was recorded at 450 nm. Then, the data were normalized by dividing the concentration of insulin by the total concentration of proteins, which was calculated using the Bradford method, and the results are shown as nanogram per milligram of protein.

Proinsulin release

To measure the amount of proinsulin, a human-specific ELISA kit was used; the absorbance of the sample was quantified at 450 nm with an ELISA reader according to manufacturer's instructions. Then, the data were normalized by dividing the concentration of proinsulin by the total concentration of proteins, and the results are exhibited as picomole per milligram of protein.

C-peptide release

Twenty-four hours postinduction, the culture supernatant was collected and the C-peptide content measured by the chemiluminescence assay at 450 nm using an ELISA reader according to the manufacturer's instructions. Data were normalized by dividing the concentration of C-peptide by the total concentration of proteins, and the results are shown as picomole per milligram of protein.

Measurement of viability of PaTu cell line

Mitochondrial activity assay

The viability of cultured cells was assessed using the MTT assay. After 24 hours of incubation, the cells were washed twice using phosphate buffer. Subsequently, 50 µL of MTT solution was added and the cells reincubated for 3–4 hours at 37°C in a 5% CO_2 humidified atmosphere. Finally, 150 µL of dimethyl sulfoxide solution was added and the absorbance determined at 570 nm using an ELISA reader. The viability

of the treatment groups was reported as the percentage of controls, which was taken as 100%.

Mitochondrial membrane potential assay

MMP was measured in PaTu cells by monitoring the uptake of the cationic dye Rhodamine 123. Briefly, after 24 hours of treatment, Rhodamine 123 was added at a concentration of 1 μM; after 10 minutes of incubation, the supernatant was read on a spectrofluorometer. The amount of dye present in the supernatant is inversely proportional to the membrane potential of the cells. The MMP of cells in the control group was taken as 100%.

Quantification of caspase-3 and -9 activities of PaTu cell line

Caspase-3 and -9 activities were measured using colorimetric assays based on the identity of specific amino acid sequences by these caspases. The tetrapeptide substrates were labeled with the chromophore r-nitroaniline (ρNA). ρNA was released from the substrate upon cleavage by caspase and produced a yellow color, the intensity of which was monitored using an ELISA reader at 405 nm. The amount of caspase activity present in the sample is proportional to the intensity of yellow color produced upon cleavage.[24] Briefly, the treated cells were lysed in the supplied lysis buffer and were incubated on ice for 10 minutes. The whole cell lysates were incubated in caspase buffer (100 mM HEPES, pH 7.4, 20% glycerol, 0.5 mM ethylenediaminetetraacetic acid [EDTA], 5 mM dithiothreitol) containing 100 mM of caspase-3 and -9-specific substrates (N-acetyl-Asp-Glu-Val-Asp-p-nitroanilide [Ac-DEVD-ρNA] and N-acetyl-Leu-Glu-His-Asp-p-nitroanilide [Ac-LEHD-ρNA], respectively) for 4 hours at 37°C. Then, absorbance was measured at 405 nm. The caspase-3 and -9 activities of the treatment groups were normalized using the the protein concentration and reported as the percentage of controls, which was taken as 100%.

Evaluation of total thiol molecules levels in PaTu cell line

TTM in the control and treatment groups were spectrophotometrically measured at 412 nm using 5,5′-dithiobis-(2-nitrobenzoic acid) (DTNB), as has been previously reported in detail.[25] In brief, 50 μL of cell homogenate was taken; to this 1 mL of Tris-EDTA buffer was added, followed by measuring the absorbance at 412 nm. Then to each well, 20 μL of DTNB (10 mM in methanol) was added. After incubation for 15 minutes, the sample absorbance was again recorded against blank DTNB. Data are shown in millimolar.

Fluorescence microscopic analysis of cell death/apoptosis using AO/EB double staining

For the analysis of cell death/apoptosis, the AO/EB double staining method was used.[26] In this regard, after 24 hours of incubation, 200 μL of dye mixture (100 μL of 100 mg/mL AO and 100 μL of 100 mg/mL EB in distilled water) was added to each well. The suspension was immediately (fast uptake) examined using fluorescence microscopy (Olympus BX51; Olympus Corporation, Tokyo, Japan) at ×20 magnification. Quantification of viable and dead cells, according to percentage of fluorescence intensity of AO/EB, was performed via ImageJ software.

Quantification of apoptotic genes by real-time PCR

To investigate the molecular mechanisms of apoptosis in PaTu cells, the expression levels of 15 apoptosis-related genes were examined by quantitative real-time reverse transcription PCR (Table 1). In this regard, after 24 hours of incubation, cells were trypsinized and centrifuged for 5 minutes at 300× *g* to allow the cells to pellet. The pellets were washed three times with sterile phosphate-buffered saline for RNA isolation. Total RNA was extracted from the cultured cells using TRIzol reagent according to the user's manual; the concentration of RNA was quantified spectrophotometrically. The genomic DNA was removed using DNase I, RNase-free kit (Fermentas, Glen Burnie, MD, USA); on the other hand, complementary DNA was reverse transcribed using the iScript cDNA Synthesis Kit. Primer pairs were used as given in Table 1, with *GAPDH* as the internal control. Quantitative real-time PCR was performed using the SYBR green master mix on an ABI prism 7300 sequence detector (Applied Biosystems, Foster City, CA, USA). Cycle number (C_t) of each reaction was calculated from the amplification curve to determine the relative gene expression using the comparative cycle threshold method.[27] $2^{-\Delta\Delta C_t}$ was used for relative gene expression analysis. All C_t values calculated from the target genes were calibrated using that from the untreated control cells.

Statistical analysis

All independent experiments were repeated four times. Data are presented as mean ± standard error of mean. One-way analysis of variance (ANOVA) and Tukey's multi-comparison tests were carried out using Stats-Direct version 3.0.171 to determine the statistical differences. The level of significance was considered at $P<0.05$. Also, the IC_{50} of DZ and regression were performed with 95% confidence intervals.

Table 1 Intrinsic and extrinsic pathway proteins, abbreviations, accession numbers, and primers used for real-time RT-PCR

Gene name	Gene symbol	Accession number	Primer sequence (5′–3′)
Intrinsic pathway proteins			
BCL2-associated X protein	*BAX*	NM_001291428	F: AACTGATCAGAACCATCATGGGC R: CTTGGATCCAGCCCAACAGCC
B-cell CLL/lymphoma 2	*BCL2*	NM_000633	F: TATAAGCTGTCGCAGAGGGGCTAC R: TGGGAGGAGAAGATGCCCGGT
Cytochrome c, somatic	*CYCS*	NM_018947.5	F: TCCCAGTCACTACTTCCTTCCT R: CAACACTTGGCTGTAGCAATG
Caspase-3, apoptosis-related cysteine peptidase	*CASP3*	NM_004346	F: ACTTTTCATTATTCAGGCCTGCCG R: CATACAAGAAGTCGGCCTCCAC
Caspase-9, apoptosis-related cysteine peptidase	*CASP9*	NM_001229	F: ACCCCAAAGCTTTCCTGCC R: TCTGTCACTGGCAGAGAAAGAGCA
Tumor protein p53	*TP53*	NM_000546	F: CATGTGCTCAAGACTGGCGCTAA R: CGCTCCCAGCCCGAACGCAA
Baculoviral IAP repeat containing 5	*BIRC5*	NM_001012270	F: GATTAGCCTCTGTCTCGGTG R: ACAAAGTTCTGCTCAGGGTG
Extrinsic pathway proteins			
Caspase-8, apoptosis-related cysteine peptidase	*CASP8*	NM_001080124	F: GGATGATGACATGAACCTGCTGG R: TTGTTGATTTGGGCACAGACTCTTT
Fas cell surface death receptor	*FAS*	NM_000043	F: GAAGCGTATGACACATTGATTAAAGATCTC R: CACTCTAGACCAAGCTTTGGATTTCATTT
TNF receptor-associated factor 2	*TRAF2*	NM_021138	F: CGTGCAGAGCGGCCTAGACCT R: CAGCTCGCGCAGGAGCTC
Tumor necrosis factor receptor superfamily, member 1A	*TNFRSF1A* (*TNFR1*)	NM_001065	F: CATTATTGGAGTGAAAACCTTT R: TGGCAGGTGCACACGGTGTT
Fas (TNFRSF6)-associated via death domain	*FADD*	NM_003824	F: GCTCTTGTCGATTTCCTGTAGTGAATC R: TCTGTCCTCGGCTCGCTGG
Fas ligand (TNF superfamily, member 6)	*FASLG*	NM_000639	F: CAACAGGGTCCCGTCCTTGACA R: AGCTGGCACTGCTGTCCACCC
Tumor necrosis factor receptor superfamily, member 10a	*TNFRSF10A* (*DR4*)	NM_003844.3	F: AGTAACAAATTCCATAAACACAATTAGC R: GACATGGTTGTCAGGACGAGCTAG
CASP8 and FADD-like apoptosis regulator	*CFLAR* (*FLIP*)	NM_001127183	F: TCTGGAGGAGAAGAACTTTGTG R: TGGCAGTGTAGTAGCTGTCGT
Glyceraldehyde-3-phosphate dehydrogenase	*GAPDH*	NM_001256799	F: GATGCTGCGCCTGCGGTAGA R: CATTGCTGATGATCTTGAGGCTGTT

Abbreviations: RT, reverse transcription; PCR, polymerase chain reaction.

Results

Determination of IC_{50} of diazinon

As shown in Figure 1, MTT assay was used to calculate the concentration of DZ, which could decrease viability by 50%. It was shown that the mitochondrial activity of PaTu cells decreased with increasing concentrations of DZ after 24 hours of exposure in comparison with untreated samples (control group). According to the obtained results, the IC_{50} of DZ was determined to be 1,300 µM.

Optimization of MgO and Se NPs concentrations

As shown in Figure 2A and B, concentration-dependent effects of MgO and Se NPs on viability of PaTu cells were observed. In case of MgO NPs, by increasing the concentration,

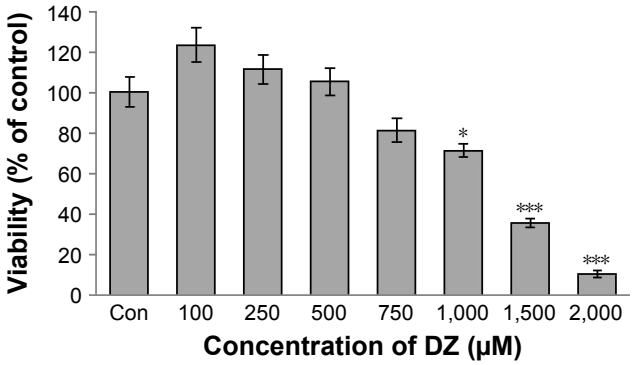

Figure 1 The inhibitory effects of cell viability on treatment with various concentrations of DZ in the PaTu cell line compared to untreated sample (Con).
Notes: The median inhibitory concentration (IC_{50}) of DZ was 1,300 µM. Results are expressed as mean ± SEM from three independent experiments. *$P<0.05$ and ***$P<0.001$ indicate statistically significant differences between the mean of values obtained with treated vs untreated cells.
Abbreviations: Con, control; DZ, diazinon; SEM, standard error of mean.

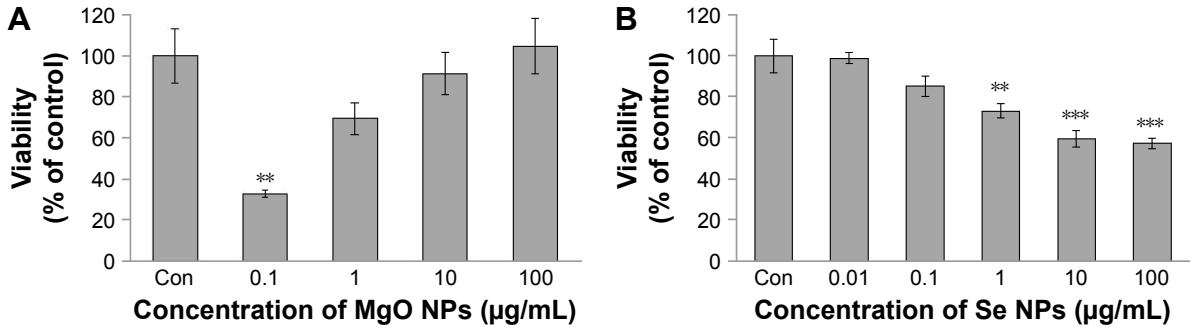

Figure 2 Effects of various concentrations of MgO NPs (**A**) and Se NPs (**B**) on cell viability in the PaTu cell line compared to untreated sample (Con).
Notes: The nontoxic concentrations of MgO and Se NPs as selective concentrations for counteraction of DZ-induced cytotoxicity in PaTu cells were 100 and 0.01 µg/mL, respectively. Results are expressed as mean ± SEM from three independent experiments. $^{**}P<0.01$ and $^{***}P<0.001$ indicate statistically significant differences between the mean of values obtained with treated vs untreated cells.
Abbreviations: Con, control; DZ, diazinon; MgO NPs, magnesium oxide nanoparticles; Se NPs, selenium nanoparticles; SEM, standard error of mean.

the viability of the cells increased, but in the Se NPs, by increasing the concentration, the viability of the cells decreased when compared with untreated samples (control group). Accordingly, in the rest of the experiments, we evaluated the effect of 100 and 0.01 µg/mL nontoxic concentrations of MgO and Se NPs, respectively, to counteract DZ-induced cytotoxicity in PaTu cells.

Determination of physiological function of PaTu cell line

Insulin release

As can be seen in Figure 3A, the release of insulin substantially decreased in the DZ group compared to control group ($P<0.01$). In comparison with DZ group, using MgO and Se NPs and their combination in the presence of DZ could increase the levels of insulin release ($P<0.01$, $P<0.001$, and $P<0.05$, respectively), and this reached a value close to that of the control group.

Proinsulin release

The effect of DZ and NPs on the release of proinsulin is shown in Figure 3B. In comparison with the control group, PaTu cells exposed to the DZ at a concentration of 1,300 µM showed a significant decline in proinsulin level, $P<0.01$. The groups that were treated with MgO and Se NPs and their combination showed a significant

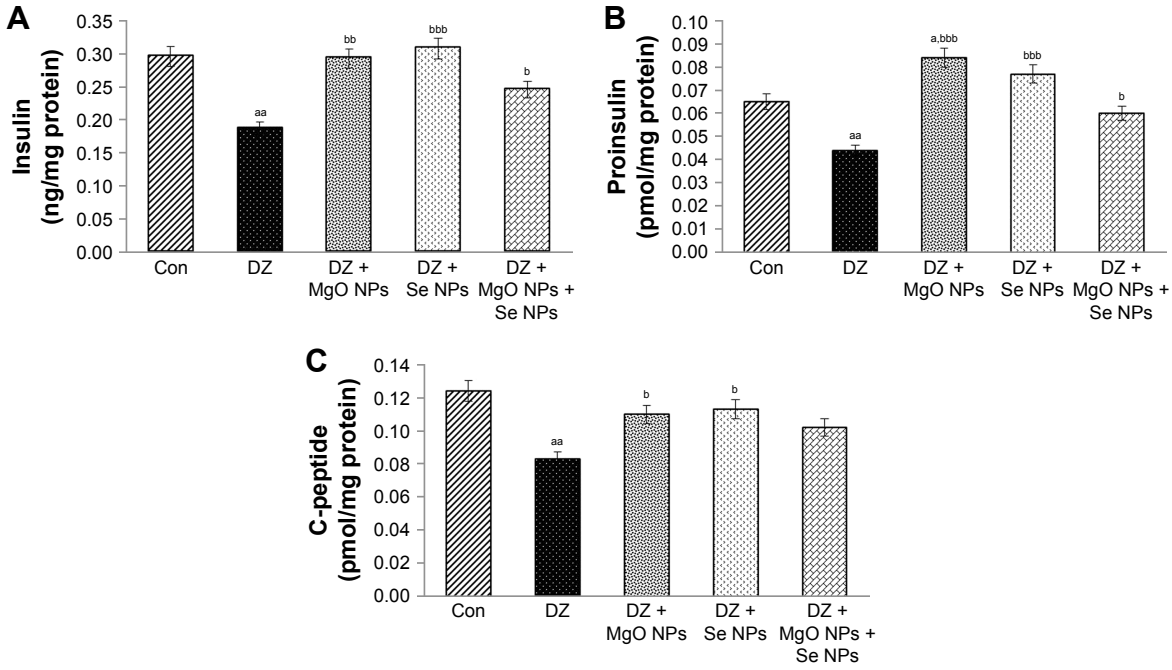

Figure 3 Effects of MgO NPs, Se NPs, and their combination on releasing insulin (**A**), proinsulin (**B**), and C-peptide (**C**) in the PaTu cell line in the presence of DZ.
Notes: Data are expressed as mean ± SEM. Significantly different from control at $^{a}P<0.05$, $^{aa}P<0.01$. Significantly different from DZ at $^{b}P<0.05$, $^{bb}P<0.01$, $^{bbb}P<0.001$.
Abbreviations: Con, control; DZ, diazinon; MgO NPs, magnesium oxide nanoparticles; Se NPs, selenium nanoparticles; SEM, standard error of mean.

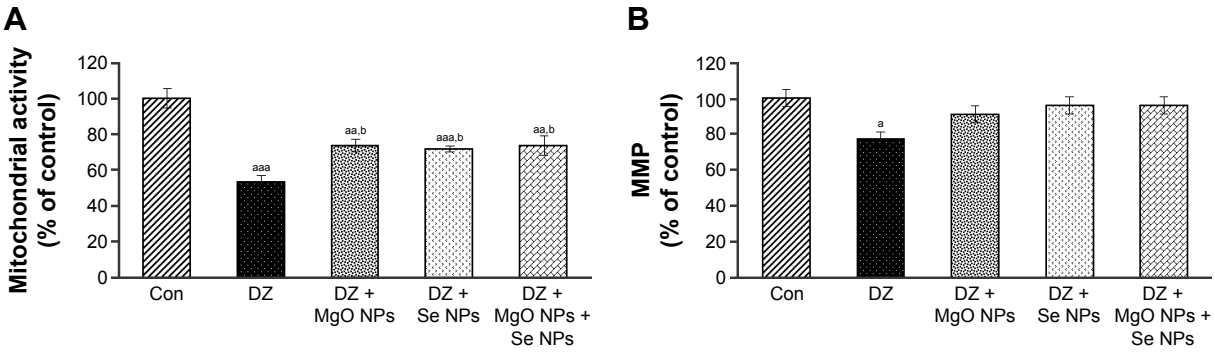

Figure 4 Effects of MgO NPs, Se NPs, and their combination on mitochondrial activity (**A**) and MMP (**B**) in the PaTu cell line in the presence of DZ.
Notes: Data are expressed as mean ± SEM. Significantly different from control at $^{a}P<0.05$, $^{aa}P<0.01$, $^{aaa}P<0.001$. Significantly different from DZ at $^{b}P<0.05$.
Abbreviations: Con, control; DZ, diazinon; MgO NPs, magnesium oxide nanoparticles; Se NPs, selenium nanoparticles; MMP, mitochondrial membrane potential; SEM, standard error of mean.

rise in proinsulin secretion when compared to DZ group ($P<0.001$, $P<0.001$, and $P<0.05$, respectively). This rise in proinsulin secretion was more noticeable in the MgO NPs group, which was also significant in comparison to control group ($P<0.05$).

C-peptide release

As shown in Figure 3C, the release of C-peptide considerably decreased in the DZ group when compared to control group ($P<0.01$). An increase in C-peptide release was observed in all treatment groups with NPs compared to the DZ group; however, this increase was significant only in MgO and Se NPs groups ($P<0.05$). In combination of MgO and Se NPs, no significant improvement in the release of C-peptide was observed as compared with DZ, the level of C-peptide was still lower than the control group.

Evaluation of viability of PaTu cell line

Mitochondrial activity

The effect of DZ and NPs on mitochondrial activity of PaTu cells is shown in Figure 4A. As illustrated in this Figure 4A, in comparison with control group (54% vs 100%), the DZ group showed a 46% decrease ($P<0.001$) in the percentage of mitochondrial activity of cells. In contrast, the groups that were treated with MgO and Se NPs and their combination showed an apparent increase in mitochondrial activity when compared to the DZ group (74%, 72%, and 74%, respectively, [$P<0.05$]); however, this increase was still lower than that in the control group ($P<0.01$, $P<0.001$, and $P<0.01$, respectively).

Mitochondrial membrane potential

DZ exposure caused a significant decline (23%, $P<0.05$) in the MMP of the cells. It was measured as percentage of control (Figure 4B). The MMP levels of groups that were treated with MgO and Se NPs and their combination demonstrated a considerable increase in comparison with DZ, but it did not show a significant difference when compared with control. The MMP of the cells in the control group was taken as 100%.

Quantification of caspase-3 and -9 activities of PaTu cell line

Figure 5 shows that the activity of caspase-3 and -9 was boosted in the DZ group compared to the control group ($P<0.05$ and $P<0.01$, respectively). On the contrary,

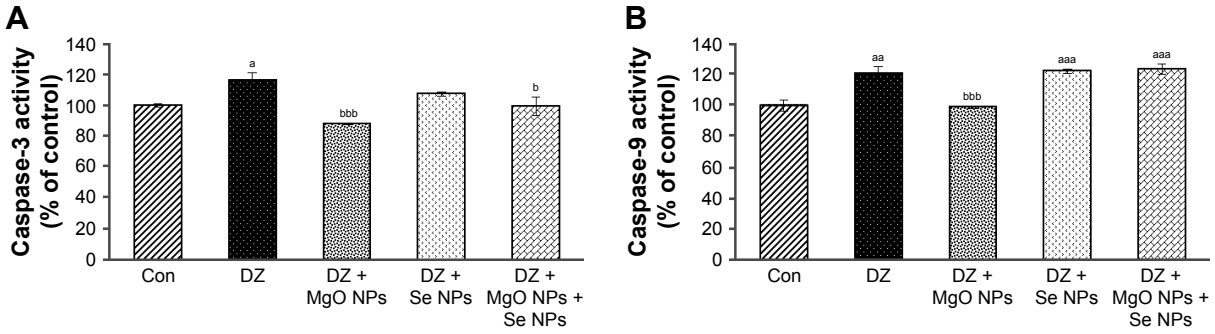

Figure 5 Effects of MgO NPs, Se NPs, and their combination on caspase-3 (**A**) and -9 activities (**B**) in the PaTu cell line in the presence of DZ.
Notes: Data are expressed as mean ± SEM. Significantly different from control at $^{a}P<0.05$, $^{aa}P<0.01$, $^{aaa}P<0.001$. Significantly different from DZ at $^{b}P<0.05$, $^{bbb}P<0.001$.
Abbreviations: Con, control; DZ, diazinon; MgO NPs, magnesium oxide nanoparticles; Se NPs, selenium nanoparticles; SEM, standard error of mean.

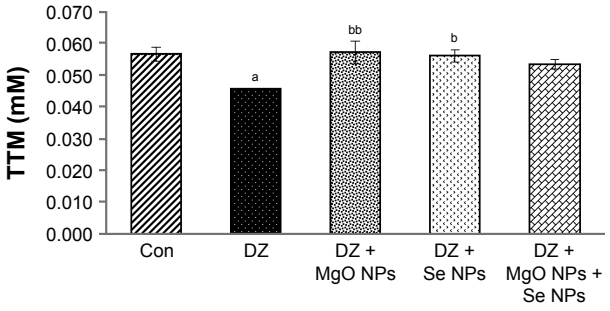

Figure 6 Effects of MgO NPs, Se NPs, and their combination on TTM levels in the PaTu cell line in the presence of DZ.
Notes: Data are expressed as mean ± SEM. Significantly different from control at $^{a}P<0.05$. Significantly different from DZ at $^{b}P<0.05$, $^{bb}P<0.01$.
Abbreviations: Con, control; DZ, diazinon; MgO NPs, magnesium oxide nanoparticles; Se NPs, selenium nanoparticles; TTM, total thiol molecules; SEM, standard error of mean.

application of MgO NPs led to a decrease of caspase-3 and -9 activities in treatment groups in comparison with the DZ group ($P<0.001$). However, the group that was treated with Se NPs showed no significant effect in lowering caspase-3 and -9 activities compared with DZ group, and with regard to caspase-9, the percentage of enzyme activity in this group was still significantly higher than that in the control group ($P<0.001$).

Determination of total thiol molecules levels in PaTu cell line

The data illustrated in Figure 6 represented the effect of DZ and NPs on the quantity of TTM in PaTu cell line. As shown, using DZ resulted in a significant reduction ($P<0.05$) in the TTM level compared to the control group. Using NPs, a general rise in the level of TTM in PaTu cell line was observed in comparison to DZ group, but this difference was found to be statistically significant only in the MgO and Se NPs groups ($P<0.01$ and $P<0.05$, respectively).

Morphological identification of cell death

The results obtained with the AO/EB staining of PaTu cells exposed for 24 hours to DZ and NPs are shown in Figure 7. As seen, most of the untreated control cells were characterized by a bright green nucleus with uniform intensity and slight uptake of EB, whereas the cells treated with DZ were orange red in appearance and showed obvious nuclear disintegration after 24 hours of treatment. Fluorescence microscopic images clearly revealed morphological alterations of the DZ-treated cells compared to the untreated control cells. As can be seen from Figure 7, there is a different percentage of fluorescence intensity of AO/EB for the DZ-treated

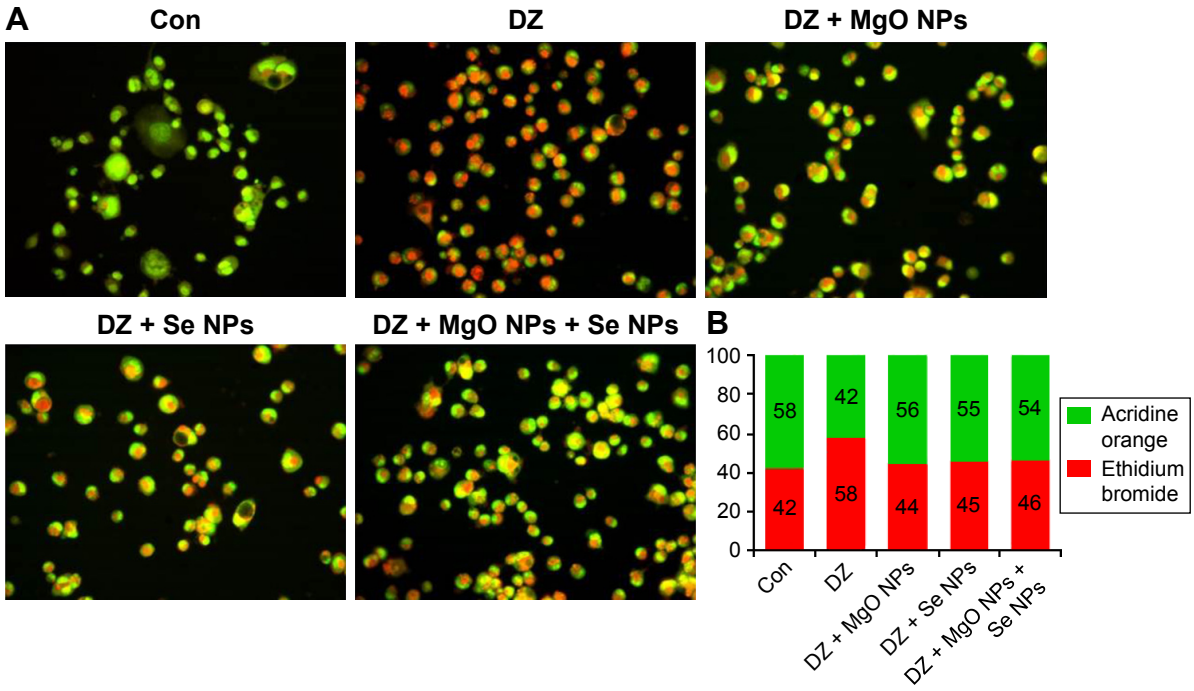

Figure 7 (**A**) Representative fluorescence microscopic images of PaTu cell line double stained with AO and EB after 24 hours of exposure to articles MgO NPs, Se NPs, and their combination in the presence of DZ. (**B**) Quantification of viable and dead cells according to percentage of fluorescence intensity of AO/EB.
Notes: (**A**) Viable cells appear uniformly green; early apoptotic cells show characteristic loss of membrane integrity and chromatin condensation, stain bright green to yellow; late apoptotic cells incorporate EB and therefore stain yellow orange and show condensed and often fragmented nuclei; necrotic cells are orange red in appearance. Images of the fields were acquired at a magnification of ×20. (**B**) AO is a vital dye and stains both live and dead cells, but EB stains only cells that have lost membrane integrity. So, an increase in the percentage of EB-stained cells indicates an increase in cell damage (apoptosis and necrosis).
Abbreviations: Con, control; DZ, diazinon; MgO NPs, magnesium oxide nanoparticles; Se NPs, selenium nanoparticles; AO, acridine orange; EB, ethidium bromide; NPs, nanoparticles.

Table 2 Relative mRNA expression using real-time PCR for expression of intrinsic and extrinsic pathway proteins in PaTu cells exposed 24 hours to DZ and NPs compared to nontreated control cells

Gene symbol	Experimental groups (relative fold change ± SEM)			
	DZ	NPs-treated groups		
		DZ + MgO	DZ + Se	DZ + MgO + Se
Intrinsic pathway proteins				
BIRC5	0.86±0.04	6.28±0.31*	6.73±0.34*	6.68±0.33*
BCL2	0.59±0.03	1.73±0.09*	2.73±0.14*	1.58±0.08*
BAX	5.46±0.27	2.89±0.15*	0.17±0.01*	0.15±0.01*
CYCS	68.12±3.41	4.11±0.21*	58.49±2.93	47.84±2.39**
CASP3	1.64±0.08	1.26±0.06***	1.55±0.08	1.14±0.06**
CASP9	5.72±0.29	1.97±0.10*	5.54±0.28	5.56±0.28
TP53	1.53±0.08	0.70±0.04*	1.42±0.07	0.86±0.04*
Extrinsic pathway proteins				
CASP8	1.45±0.07	1.13±0.06***	1.05±0.05**	1.33±0.07
FAS	2.16±0.11	0.52±0.03*	0.93±0.05*	1.61±0.08**
TRAF2	2.31±0.12	0.86±0.04*	0.84±0.04*	1.97±0.10
TNFRSF1A (*TNFR1*)	1.55±0.08	0.38±0.02*	0.68±0.03*	0.68±0.03*
FADD	0.67±0.03	0.34±0.02*	0.91±0.05**	0.48±0.02***
FASLG	0.69±0.04	0.57±0.03	0.58±0.03	0.47±0.02**
TNFRSF10A (*DR4*)	0.52±0.03	0.37±0.02***	0.74±0.04**	0.52±0.03
CFLAR (*FLIP*)	1.78±0.09	1.30±0.07***	2.87±0.14*	0.81±0.04*

Notes: *GAPDH* is the housekeeping gene control. Results are expressed as mean ± SEM from three independent experiments. *$P<0.001$, **$P<0.01$, and ***$P<0.05$ indicate significantly different from DZ.

Abbreviations: SEM, standard error of mean; DZ, diazinon; NPs, nanoparticles; MgO, magnesium oxide; Se, selenium; PCR, polymerase chain reaction.

cells compared to the control or nontreated cells (% of AO: 42 vs 58, % of EB: 58 vs 42).

It was shown that cell incubation with DZ resulted in the reduction of cell viability and similar increase of apoptosis and necrosis. In contrast, NPs-treated (MgO and Se NPs and their combination) groups displayed lower intensity of EB compared to DZ group (44, 45, and 46 vs 58), revealing a decrease in the numbers of apoptotic and necrotic cells. Interestingly, there were no significant differences in intensity of AO (green viable cells) in comparison with control group (56, 55, and 54 vs 58).

Expression profiles of apoptotic genes in PaTu cell line

To investigate the molecular mechanism of apoptosis in PaTu cell line, the expression levels of 15 apoptosis-related genes were examined (Table 2). The expression levels of these 15 genes were analyzed by real-time PCR to evaluate the effect of DZ and NPs on the expression of intrinsic and extrinsic pathway proteins (7 and 8 genes, respectively). The analysis of data showed that the changes in the gene expression induced by DZ were significantly different in the PaTu cells compared to changes induced by NPs. Two genes of inhibitors of apoptosis, *BIRC5* and *BCL2*, were upregulated after treatment of cells by MgO and Se NPs and their combination (>7-fold and >2.67-fold for *BIRC5* and *BCL2*, respectively). In contrast, treatment of cells with NPs downregulated the genes involved in the intrinsic pathway of apoptosis, such as *BAX*, *CYCS*, *CASP3*, *CASP9*, and *TP53*, compared to DZ-treated cells. The expression changes of these genes were significantly different in MgO NPs and combination groups when compared with DZ group. Simultaneously, the expression levels of the eight genes involved in the extrinsic pathway of apoptosis, such as *CASP8*, *FAS*, *TRAF2*, *TNFRSF1A* (*TNFR1*), *FADD*, *FASLG*, *TNFRSF10A* (*DR4*), and *CFLAR* (*FLIP*), were evaluated. As seen in the Table 2, MgO and Se NPs exert their effects in part by modulation and downregulation of some genes of extrinsic pathway proteins such as *CASP8*, *FAS*, *TRAF2*, *TNFRSF1A* (*TNFR1*), and *DR4*. Considerably, *FADD* and *FLIP* were significantly upregulated in Se NPs group, whereas they were downregulated in MgO and combination groups in comparison to DZ group. In the case of *FASLG*, significant expression changes were observed only in the combination group and not in the DZ group.

Discussion

OP compounds such as DZ are potent inhibitors of the enzyme AChE.[1,28] Inhibition of AChE during both acute and chronic toxicity of these compounds plays a key role in the induction of disorders. For example, these factors lead to the development of hyperglycemic and hemostatic disorders related to glucose metabolism and can be regarded as

precursors to diabetes.[1,29] On the other hand, oxidative stress is considered as one of the pivotal factors in the development of diabetes complications, and its relation to some OP pesticides such as malathion and DZ has been reported.[30,31] These studies have indicated that the acute and chronic toxicities of OPs were closely related to the increased production of ROS and lipid peroxidation.

NPs can be synthesize chemically or biologically and may have several unknown effects, one of which is a positive/protective effect on various cells. They could penetrate into a different place and have protective effects against oxidative stress-induced cell death through different mechanisms.[32] Since the related mechanisms are not well understood, especially in apoptosis and mitochondria toxicity, in this study, we investigated the protective mechanisms of MgO and Se NPs against DZ-induced cytotoxicity in the PaTu cell line.

Our results demonstrated that using MgO and Se NPs could improve the release of insulin, proinsulin, and C-peptide (all of which were inhibited after exposure to DZ), one of the main functions of the PaTu cells. In this area of research, previous studies have shown that metal oxide NPs, including CeO_2, Y_2O_3, ZnO, and MgO, were capable of enhancing cell survival and function under conditions of oxidative stress;[33–37] the reason for increasing insulin by metal oxide NPs was justified by their antioxidant property.[38] In addition, it was demonstrated that using metal oxide NPs induces a cascade of protein phosphorylation due to increase of ATP/ADP ratio that finally leads to secretion of insulin.

In addition, DZ can induce mitochondrial damage, such as the loss of MMP, and lead to a decrease of mitochondrial activity in human PaTu cells, which suggests that mitochondrial damage might play a role in DZ-induced cell death. Mitochondrial potential loss triggers the caspase cascade leading to increased apoptosis. Therefore, the caspase enzyme activity, as one of the mechanisms for justifying the apoptosis,[39] was assessed in this study by measuring caspase-3 and -9 activities. On the basis of our results, it was hypothesized that using MgO NPs with the potential to prevent caspase enzyme activity could enable PaTu cells survive the cytotoxicity of DZ exposure.

OP-induced cell death specially by DZ has been described generally in different cell types, including ovarian follicular cells, cardiac muscle cells, NTera2-D1 cells, peripheral blood lymphocytes, and skeletal muscles.[8,40–43] In this report, we demonstrated that the type of cell death induced by DZ is predominantly apoptotic, as determined by MTT and MMP, caspase-3 and -9 activities, and AO/EB staining assays. Moreover, to investigate in greater detail the factors that are possibly responsible for apoptosis, the expression levels of 15 apoptosis-related genes were analyzed by real-time PCR.

Depending on the trigger of the cell death program, the basic mechanism of apoptosis has been divided into intrinsic mitochondrial and extrinsic death receptor pathways.[44] The intrinsic apoptotic pathway is activated by intracellular events, depends on the release of proapoptotic and antiapoptotic factors, such as the Bcl-2 family proteins, cytochrome c, Apaf-1, Endo G, and procaspase-9 proteins from mitochondria to cytosol, and leads to activation of caspase-9. The extrinsic apoptotic pathway is initiated by the binding of an extracellular death ligand to its cell surface death receptors, including Fas/CD95, DR4, and DR5, influences the intracellular apoptotic adaptor FADD protein, and then proceeds through caspase-8 to activate executor caspases. While inhibition of Bcl-2-mediated intrinsic pathway results in the activation of caspases 9 and 3, death receptor-mediated extrinsic pathway involves caspases 10 and 8 in inducing apoptosis. Notably, both pathways converge at caspase-3, leading to activation of other proteases.[44–48] Accordingly, caspases are the key effector molecules in both apoptotic pathways and are potential targets for pharmacological modulation of cell death. The discovery of drugs that selectively block caspases in both the intrinsic and extrinsic pathways should help control the cytotoxicity of OP compounds such as DZ. Our results demonstrated that DZ significantly increased the expressions of caspase-9, caspase-8, and caspase-3 genes (5.72-fold, 1.45-fold, and 1.64-fold, respectively) after 24 hours of treatment, and cotreatment of cells with MgO NPs alone and in combination with Se NPs through specific inhibition of caspase genes significantly prevented DZ-induced cell apoptosis (Table 2).

In conclusion, these data provide evidence supporting the fact that treatment of PaTu cells with NPs modulate DZ-induced apoptosis through the changes in the expression of genes involved in both intrinsic and extrinsic caspase-dependent pathways.

Unexpectedly, there was no clear indication of synergistic interactions when MgO and Se NPs were used in combination. This observation indicates that either the maximal modulation possible is achieved with a single agent or that these agents modulate DZ-induced apoptosis through a common pathway.

Conclusion

Taken together, the results of the current study using MgO and Se NPs on PaTu cell line in terms of increasing the viability/function and decreasing oxidative stress/apoptosis

reveal the possible molecular mechanisms and signaling pathways of the antiapoptotic properties of these NPs against cytotoxicity of DZ exposure for human pancreatic cancer cell line. It is noteworthy to mention that all NPs owing to their small size and ability to pass through cell membranes and biological barriers might be toxic if used in nonoptimized doses.[48] Therefore, further care should be taken while doing in vivo animal studies and human studies to ascertain the safety and efficacy of these NPs.[49,50]

Acknowledgment

The authors wish to thank Artesh University of Medical Sciences that helped in providing some of needed materials in support of the study of the first author.

Disclosure

M Abdollahi received a Tehran University of Medical Sciences and Iran National Science Foundation Self-Directed Grant. The authors report no conflicts of interest in this work.

References

1. Aggarwal V, Deng X, Tuli A, Goh KS. Diazinon-chemistry and environmental fate: a California perspective. *Rev Environ Contam Toxicol*. 2013;223:107–140.
2. Colović MB, Krstić DZ, Lazarević-Pašti TD, Bondžić AM, Vasić VM. Acetylcholinesterase inhibitors: pharmacology and toxicology. *Curr Neuropharmacol*. 2013;11(3):315–335.
3. Pizzurro DM, Dao K, Costa LG. Diazinon and diazoxon impair the ability of astrocytes to foster neurite outgrowth in primary hippocampal neurons. *Toxicol Appl Pharmacol*. 2014;274(3):372–382.
4. Pizzurro DM, Dao K, Costa LG. Astrocytes protect against diazinon- and diazoxon-induced inhibition of neurite outgrowth by regulating neuronal glutathione. *Toxicol*. 2014;318:59–68.
5. Zafiropoulos A, Tsarouhas K, Tsitsimpikou C, et al. Cardiotoxicity in rabbits after a low-level exposure to diazinon, propoxur, and chlorpyrifos. *Hum Exp Toxicol*. 2014;33(12):1241–1252.
6. Mostafalou S, Abdollahi M. Pesticides and human chronic diseases: evidences, mechanisms, and perspectives. *Toxicol Appl Pharmacol*. 2013;268(2):157–177.
7. Boussabbeh M, Ben Salem I, Hamdi M, Ben Fradj S, Abid-Essefi S, Bacha H. Diazinon, an organophosphate pesticide, induces oxidative stress and genotoxicity in cells deriving from large intestine. *Environ Sci Pollut Res Int*. 2016;23(3):2882–2889.
8. Aluigi MG, Guida C, Falugi C. Apoptosis as a specific biomarker of diazinon toxicity in NTera2-D1 cells. *Chem Biol Interact*. 2010;187(1–3):299–303.
9. Soltaninejad K, Abdollahi M. Current opinion on the science of organophosphate pesticides and toxic stress: a systematic review. *Med Sci Monit*. 2009;15(3):RA75–RA90.
10. Skelin M, Rupnik M, Cencic A. Pancreatic beta cell lines and their applications in diabetes mellitus research. *ALTEX*. 2010;27(2):105–113.
11. Elsässer HP, Lehr U, Agricola B, Kern HF. Structural analysis of a new highly metastatic cell line PaTu 8902 from a primary human pancreatic adenocarcinoma. *Virchows Arch B Cell Pathol Incl Mol Pathol*. 1993;64(4):201–207.
12. Sushma NJ, Prathyusha D, Swathi G, et al. Facile approach to synthesize magnesium oxide nanoparticles by using *Clitoria ternatea* – characterization and in vitro antioxidant studies. *Appl Nanosci*. 2016;6(3):437–444.
13. Heydary V, Navaei-Nigjeh M, Rahimifard M, Mohammadirad A, Baeeri M, Abdollahi M. Biochemical and molecular evidences on the protection by magnesium oxide nanoparticles of chlorpyrifos-induced apoptosis in human lymphocytes. *J Res Med Sci*. 2015;20(11):1021–1031.
14. Shafiee H, Mohammadi H, Rezayat SM, et al. Prevention of malathion-induced depletion of cardiac cells mitochondrial energy and free radical damage by a magnetic magnesium-carrying nanoparticle. *Toxicol Mech Methods*. 2010;20(9):538–543.
15. Rezvanfar MA, Rezvanfar MA, Shahverdi AR, et al. Protection of cisplatin-induced spermatotoxicity, DNA damage and chromatin abnormality by selenium nano-particles. *Toxicol Appl Pharmacol*. 2013;266(3):356–365.
16. Fakhri-Bafghi MS, Ghasemi-Niri SF, Mostafalou S, et al. Protective effect of selenium-based medicines on toxicity of three common organophosphorus compounds in human erythrocytes in vitro. *Cell J*. 2016;17(4):740–747.
17. Malhotra S, Welling MN, Mantri SB, Desai K. In vitro and in vivo antioxidant, cytotoxic, and anti-chronic inflammatory arthritic effect of selenium nanoparticles. *J Biomed Mater Res B Appl Biomater*. 2016;104(5):993–1003.
18. Fesharaki PJ, Nazari P, Shakibaie M, et al. Biosynthesis of selenium nanoparticles using Klebsiella pneumoniae and their recovery by a simple sterilization process. *Braz J Microbiol*. 2010;41(2):461–466.
19. Shakibaie M, Khorramizadeh MR, Faramarzi MA, Sabzevari O, Shahverdi AR. Biosynthesis and recovery of selenium nanoparticles and the effects on matrix metalloproteinase-2 expression. *Biotechnol Appl Biochem*. 2010;56(1):7–15.
20. Shokrzadeh M, Ahmadi A, Ramezaninejhad S, Shadboorestan A. Hesperidin, a citrus bioflavonoid, ameliorates genotoxicity-induced by diazinon in human blood lymphocytes. *Drug Res*. 2015;65(2):57–60.
21. Pourkhalili N, Pournourmohammadi S, Rahimi F, et al. Comparative effects of calcium channel blockers, autonomic nervous system blockers, and free radical scavengers on diazinon-induced hyposecretion of insulin from isolated islets of Langerhans in rats. *Arh Hig Rada Toksikol*. 2009;60(2):157–164.
22. Ge S, Wang G, Shen Y, et al. Cytotoxic effects of MgO nanoparticles on human umbilical vein endothelial cells in vitro. *IET Nanobiotechnol*. 2011;5(2):36.
23. Shakibaie M, Shahverdi AR, Faramarzi MA, Hassanzadeh GR, Rahimi HR, Sabzevari O. Acute and subacute toxicity of novel biogenic selenium nanoparticles in mice. *Pharm Biol*. 2013;51(1):58–63.
24. Kim JY, Lim DM, Moon CI, et al. Exendin-4 protects oxidative stress-induced b-cell apoptosis through reduced JNK and GSK3b activity. *J Korean Med Sci*. 2010;25(11):1626–1632.
25. Naghizadeh B, Mansouri MT, Ghorbanzadeh B. Protective effects of crocin against streptozotocin-induced oxidative damage in rat striatum. *Acta Medica Iranica*. 2014;52(2):101–105.
26. Baskić D, Popović S, Ristić P, Arsenijević NN. Analysis of cycloheximide-induced apoptosis in human leukocytes: fluorescence microscopy using annexin V/propidium iodide versus acridin orange/ethidium bromide. *Cell Biol Int*. 2006;30(11):924–932.
27. Schmittgen TD, Livak KJ. Analyzing real-time PCR data by the comparative C (T) method. *Nat Protoc*. 2008;3(6):1101–1108.
28. Karami-Mohajeri S, Abdollahi M. Mitochondrial dysfunction and organophosphorus compounds. *Toxicol Appl Pharmacol*. 2013;270(1):39–44.
29. Teimouri F, Amirkabirian N, Esmaily H, Mohammadirad A, Aliahmadi A, Abdollahi M. Alteration of hepatic cells glucose metabolism as a non-cholinergic detoxication mechanism in counteracting diazinon-induced oxidative stress. *Hum Exp Toxicol*. 2006;25(12):697–703.
30. Pakzad M, Fouladdel S, Nili-Ahmadabadi A, et al. Sublethal exposures of diazinon alters glucose homostasis in Wistar rats: biochemical and molecular evidences of oxidative stress in adipose tissues. *Pestic Biochem Physiol*. 2013;105(1):57–61.

31. Rahimi R, Abdollahi M. A review on the mechanisms involved in hyperglycemia induced by organophosphorus pesticides. *Pestic Biochem Physiol*. 2007;88(2):115–121.
32. Hassanin KM, Abd El-Kawi SH, Hashem KS. The prospective protective effect of selenium nanoparticles against chromium-induced oxidative and cellular damage in rat thyroid. *Int J Nanomed*. 2013;8:1713–1720.
33. Pourkhalili N, Hosseini A, Nili-Ahmadabadi A, et al. Improvement of isolated rat pancreatic islets function by combination of cerium oxide nanoparticles/sodium selenite through reduction of oxidative stress. *Toxicol Mech Methods*. 2012;22(6):476–482.
34. Pourkhalili N, Hosseini A, Nili-Ahmadabadi A, et al. Biochemical and cellular evidence of the benefit of a combination of cerium oxide nanoparticles and selenium to diabetic rats. *World J Diabetes*. 2011;2(11):204–210.
35. Shoae-Hagh P, Rahimifard M, Navaei-Nigjeh M, et al. Zinc oxide nanoparticles reduce apoptosis and oxidative stress values in isolated rat pancreatic islets. *Biol Trace Elem Res*. 2014;162(1–3):262–269.
36. Navaei-Nigjeh M, Rahimifard M, Pourkhalili N, et al. Multi-organ protective effects of cerium oxide nanoparticle/selenium in diabetic rats: evidence for more efficiency of nanocerium in comparison to metal form of cerium. *Asian J Anim Vet Adv*. 2012;7(7):605–612.
37. Hosseini A, Baeeri M, Rahimifard M, et al. Antiapoptotic effects of cerium oxide and yttrium oxide nanoparticles in isolated rat pancreatic islets. *Hum Exp Toxicol*. 2013;32(5):544–553.
38. Mohseni Salehi Monfared SS, Larijani B, Abdollahi M. Islet transplantation and antioxidant management: a comprehensive review. *World J Gastroenterol*. 2009;15(10):1153–1161.
39. Leist M, Jaattela M. Four deaths and a funeral: from caspases to alternative mechanisms. *Nat Rev Mol Cell Biol*. 2001;2(8):589–598.
40. Sargazi Z, Nikravesh MR, Jalali M, Sadeghnia HR, Rahimi-Anbarkeh F. Apoptotic effect of organophosphorus insecticide diazinon on rat ovary and protective effect of vitamin E. *Iran J Toxicol*. 2016;10(2):37–44.
41. Ogutcua A, Uzunhisarciklia M, Kalenderb S, Durakc D, Bayrakdara F, Kalender Y. The effects of organophosphate insecticide diazinon on malondialdehyde levels and myocardial cells in rat heart tissue and protective role of vitamin E. *Pestic Biochem Physiol*. 2006;86(2):93–98.
42. Muranli FD, Kanev M, Ozdemir K. Genotoxic effects of diazinon on human peripheral blood lymphocytes. *Arh Hig Rada Toksikol*. 2015;66(2):153–158.
43. Pournourmohammadi S, Farzami B, Ostad SN, Azizi E, Abdollahi M. Effects of malathion subchronic exposure on rat skeletal muscle glucose metabolism. *Environ Toxicol Pharmacol*. 2005;19(1):191–196.
44. Elmore S. Apoptosis: a review of programmed cell death. *Toxicol Pathol*. 2007;35(4):495–516.
45. Caroppi P, Sinibaldi F, Fiorucci L, Santucci R. Apoptosis and human diseases: mitochondrion damage and lethal role of released cytochrome C as proapoptotic protein. *Curr Med Chem*. 2009;16(31):4058–4065.
46. Kiechle FL, Zhang X. Apoptosis: biochemical aspects and clinical implications. *Clin Chim Acta*. 2002;326(1–2):27–45.
47. Riedl SJ, Shi Y. Molecular mechanisms of caspase regulation during apoptosis. *Nat Rev Mol Cell Biol*. 2004;5(11):897–907.
48. Burz C, Berindan-Neagoe I, Balacescu O, Irimie A. Apoptosis in cancer: key molecular signaling pathways and therapy targets. *Acta Oncol*. 2009;48(6):811–821.
49. Mogharabi M, Abdollahi M, Faramarzi MA. Toxicity of nanomaterials; an undermined issue. *Daru*. 2014;22(1):59.
50. Nassiri Koopaei N, Abdollahi M. Opportunities and obstacles to the development of nanopharmaceuticals for human use. *Daru*. 2016;24(1):23.